Article ID: 1000-324X(2023)03-0350-07 **DOI:** 10.15541/jim20220386

Spectroscopic and Yellow Laser Features of Dy^{3+}: $Y_3Al_5O_{12}$ Single Crystals

YANG Jiaxue[1,2], LI Wen[1,3], WANG Yan[1,4], ZHU Zhaojie[1,4], YOU Zhenyu[1,4], LI Jianfu[1,4], TU Chaoyang[1,4]

(1. Fujian Institute of Research on the Structure of Matter, Chinese Academy of Sciences, Fuzhou 350002, China; 2. College of Chemistry, Fuzhou University, Fuzhou 350116, China; 3. School of Materials Science and Engineering, Fuzhou University, Fuzhou 350116, China; 4. Fujian Science & Technology Innovation Laboratory for Optoelectronic Information of China, Fuzhou 350108, China)

Abstract: In recent years, yellow laser crystals have raised great attentions owing to their comprehensive applications in the fields such as laser display, laser medical treatment, light detection and ranging (LIDAR), Bose-Einstein condensates, and atomic cooling and trapping. With the development of commercial blue light LD, the direct pumping of Dy^{3+} doped laser crystals has realized yellow laser based on its transition $^4F_{9/2}\rightarrow{}^6H_{13/2}$. In this work, Dy^{3+}: $Y_3Al_5O_{12}$ (Dy: YAG) crystals with 0.5%, 1.0%, 2.0%, 3.0%, and 4.0% (atomic fraction) nominal concentration of Dy^{3+} were grown using Czochralski method, the reason of crystal crack was discussed. Based on Judd-Ofelt (J-O) theory, the J-O intensity parameters and utilization, and other laser parameters of Dy: YAG crystals with different doping concentrations were evaluated. The effect of the doping concentration of Dy^{3+} on the spectroscopic performances like fluorescence branching ratio, stimulated emission cross-section, quantum efficiency, were analyzed comprehensively. Among all the five crystals, 1.0% Dy: YAG has the largest stimulated emission cross-section for 582 nm yellow emission, an intense fluorescence intensity with the 447 nm excitation, and a longer decay time of 0.823 ms. The fluorescence intensity and stimulated emission cross-section of 2.0% Dy: YAG are slightly less than that of 1.0% Dy: YAG, but the former has a higher absorption coefficient. Hence, the spectroscopic analysis results show that 1.0% and 2.0% are the suitable concentrations of Dy^{3+} ion in YAG crystal for yellow laser operation by diode pumping. The continuous wave laser with peak at 582.5 nm and the maximum output power of 166.8 μW yellow laser operation were realized in 2.0% Dy: YAG crystal.

Key words: YAG crystal; Dy^{3+}; crystal growth; fluorescence features; yellow laser

The interest in Dy^{3+} doped optical materials is rapidly growing recently, and more and more researches about different Dy^{3+}-containing materials were reported[1-5]. Dy^{3+} doped luminescent materials in the visible region are burgeoning due to peculiar emissions which differ from other RE (rare-earth) ions doped materials. Dy^{3+} is also the only RE ion with yellow emission in addition to Tb^{3+}. Because of the strong yellow emission intensity which is several times of Tb^{3+} doping at the same doping concentration and wide emission band from 565 nm to 595 nm, Dy^{3+} doped single crystals are promising in the field of all-solid-state laser[6]. Generally, a yellow laser is used for the treatment of fundus diseases and dermatological disorders in medical treatments[7-8]. 578 nm laser can be used for a Yb optical clock that matches the $^1S_0$-$^3P_0$ transition of the Yb atoms, and 589 nm yellow laser can be used as a sodium beacon laser[9-10]. Dy^{3+} shows absorption bands in both blue and UV (ultraviolet) regions that match the InGaN blue LD (laser diode). The yellow laser operation using Dy^{3+} doped single crystal was reported for the first time in 2012 and gives confidence to the researchers to focus on the yellow laser based on Dy^{3+} ion-doped crystals[11].

In recent years, all types of Dy^{3+} doped single crystals are reported, which provide a sufficient number of references for comparison of the performances among

Received date: 2022-07-05; **Revised date:** 2022-08-16; **Published online:** 2021-11-16
Foundation item: National Natural Science Foundation of China (51872286, 51832007); Fujian Science & Technology Innovation Laboratory for Optoelectronic Information of China (2021ZR204); Science and Technology Plan Leading Project of Fujian Province (2022H0043, 2020H0036); Natural Science Foundation of Jiangxi Province (20181BAB211009)
Biography: YANG Jiaxue (1995–), female, Master candidate. E-mail: yangjiaxue@fjirsm.ac.cn
杨佳雪(1995–), 女, 硕士研究生. E-mail: yangjiaxue@fjirsm.ac.cn
Corresponding author: WANG Yan, professor. E-mail: wy@fjirsm.ac.cn; TU Chaoyang, professor. E-mail: tcy@fjirsm.ac.cn
王 燕, 研究员. E-mail: wy@fjirsm.ac.cn; 涂朝阳, 研究员. E-mail: tcy@fjirsm.ac.cn

different host materials[12-17]. Unfortunately, to our best knowledge, up to now yellow laser output using Dy^{3+} activated bulk crystal (not fiber laser) as a gain medium was achieved successfully only in several host materials[11, 18-20]. $Y_3Al_5O_{12}$ (YAG) is a typical laser crystal with high mechanical strength which cannot be broken down easily during laser experiments. The higher phonon energy of YAG makes the population on $^6H_{13/2}$ level could greater extent transfer to ground state $^6H_{15/2}$ by non-radiative transitions. It is relatively easy to grow YAG crystal using the Czochralski method on account of the congruent melting property. It also has a low cost due to the relatively cheaper raw materials Y_2O_3 and Al_2O_3. The spectroscopic characteristics of 3.0% Dy^{3+}: YAG crystal under 384 nm excitation were investigated by Pan, *et al*[21]. The spectroscopic properties of 3.0% Dy^{3+}: YAG crystal grown by the micro-pulling-down method were reported by Xu[22]. In addition, Dy^{3+} doped single crystal could be applied in the display and lighting areas on account of the strong blue and yellow emissions in visible waveband, which makes the white emitting available. Yu, *et al*[23] grew the Gd^{3+}/Dy^{3+} co-doped CaF_2 crystal by the Bridgeman method and the tunable white light were obtained by changing the concentration of Gd^{3+}. The research from Xu, *et al*[24] showed Dy^{3+}/Eu^{3+} co-doped $LiLuF_4$ single crystal had good optical features and thermal stability. A white light emitting under 355 nm excitation in the Dy^{3+}: $Gd_3Sc_2Al_3O_{12}$ crystal was demonstrated by Ding, *et al*[25]. The 366 nm absorption band of Dy^{3+}: $Y_3Al_5O_{12}$ (Dy: YAG) matches the excitation wavelength of commercial GaN UV-LED chips. Compared with phosphor powders containing Dy^{3+} ion, a single crystal is free of impurity phases, has good uniformity of activated ions, which does not need epoxy resin packaging.

Dy^{3+} concentration has a great influence on the fluorescence performance of Dy^{3+} doped crystals, and it is meaningful to choose the appropriate doping concentration of Dy: YAG crystal for luminescence and laser operation. The previous researches on Dy^{3+} doped YAG single crystals always concentrated on one crystal with a specific Dy^{3+} doping concentration, and there are only a few studies on the effect of doping concentration on the spectroscopic properties. In this work, the emission spectra of different doping concentration Dy: YAG crystals were contrasted at 447 nm excitation and the spectroscopic parameters were calculated and discussed. The laser properties of Dy: YAG single crystal as laser gain medium was presented.

1 Experimental

$Y_{3-x}Dy_xAl_5O_{12}$ (x = 0.015, 0.03, 0.06, 0.09, and 0.12) polycrystalline powders were synthesized by high-temperature solid reaction method. Dy_2O_3, Y_2O_3, and Al_2O_3 were weighted and mixed according to the stoichiometric ratio and pressed into tablets for sintering. After the sintering process, they were put into an Ir crucible for crystal growth. Yttrium aluminum garnet crystals with different Dy^{3+} concentrations (0.5%, 1.0%, 2.0%, 3.0%, 4.0%, atomic fraction) were grown using the Czochralski method under a high purity N_2 atmosphere. To eliminate the defects in the crystals and release the stress, such crystals were annealed in the air. An image of as-grown crystals is presented in Fig. 1.

The Dy^{3+} concentration of the upper part of the crystals was measured by an inductively coupled plasma atomic emission spectrometer (ICP-AES, Ultima2, Jobin-Yvon). Powder X-ray diffraction (XRD) was characterized on an X-ray diffractometer (Miniflex-600, Rigaku) in step scan mode. The absorption spectra of the samples with a size of 10 mm×10 mm×1 mm were recorded by a UV-VIS-NIR spectrometer (Lamda-980, Perkin-Elmer). The emission spectra and decay curves were measured by a fluorescence spectrometer (FLS980, Edinburgh Instruments). The pump source was a diode laser with the central wavelength of 447 nm and maximum output power of 3.58 W. The laser cavity consisted of two mirror with high transmission (>96%) at 447 nm and high reflection (>99.7%). The 2.0%Dy:YAG crystal with the size of 5 mm×5 mm×10 mm was wrapped with the indium foil and put on the thermos electric cooler.

As seen in Fig. 1, there appeared bubbles and crack in 4.0%Dy: YAG crystal which was grown at first in this work. The appearance of bubbles and crack might stem from the impure polycrystalline powders. To avoid the impaction of impurity phases, we used higher purity of raw materials and extended the grinding time to make the mixture more homogeneous. High quality seed crystal was also used to inhibit the defects of crystals. Furthermore, some measurements were taken such as slowing down the rate of heating and keeping the temperature above the melting point 100 ℃ for several hours, to make sure the polycrystalline melt completely which eliminated gas bubbles effectively. Changing the temperature field around crucible could improve this situation efficiently too. To strengthen the insulation, the gap between zirconia cylindrical thermal insulation materials and crucible was filled with zirconia powders. At the same time, double-layer zirconia cylinder was used to prevent crystal cracking during annealing.

2 Results and discussion

2.1 Absorption spectra and Judd-Ofelt (J-O) analysis

Absorption spectra of Dy: YAG crystals measured at

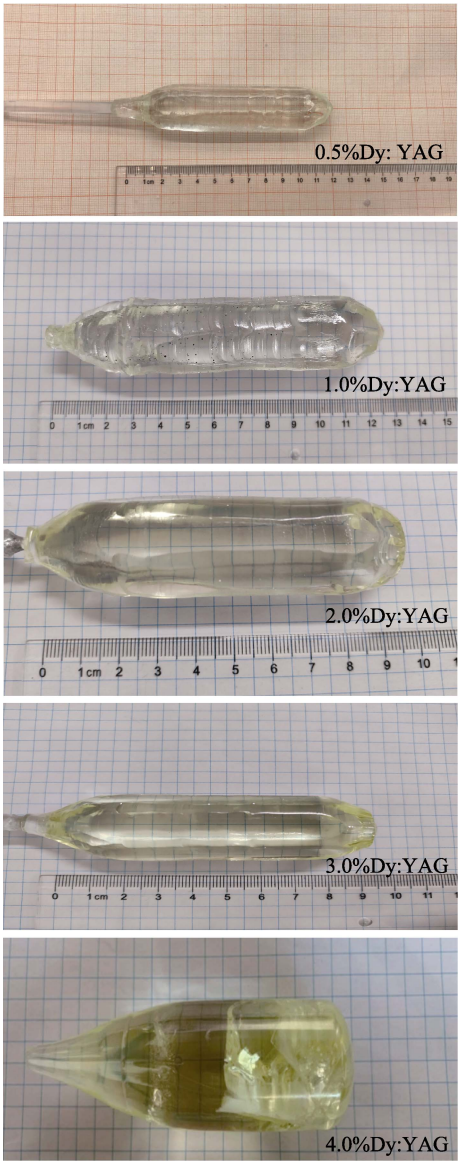

Fig. 1 Photos of the as-grown single crystals

room temperature are depicted in Fig. 2, which indicates that the absorption coefficient (α) is proportional to the Dy^{3+} concentration. With an increase in doping concentration, the peak wavelengths of absorption bands are almost unchanged. Peaks at 353, 366, 386, 447, 479, 752, 804, 897, 1073, 1291, and 1687 nm correspond to the transitions

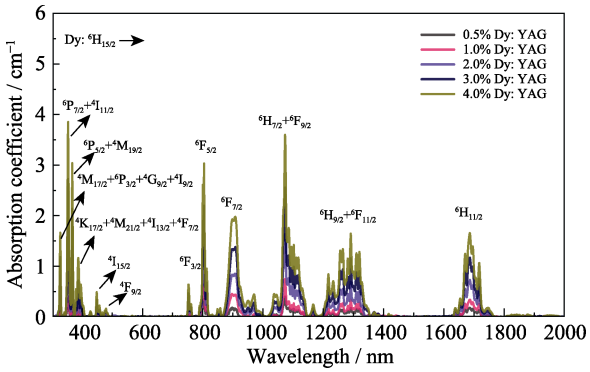

Fig. 2 Absorption spectra of Dy: YAG crystals

from the ground state $^6H_{15/2}$ to $^6P_{7/2}$+$^4I_{11/2}$, $^6P_{5/2}$+$^4M_{19/2}$, $^4K_{17/2}$+$^4M_{21/2}$+$^4F_{7/2}$+$^4I_{13/2}$, $^4I_{15/2}$, $^4F_{9/2}$, $^6F_{3/2}$, $^6F_{5/2}$, $^6F_{7/2}$, $^6H_{7/2}$+$^6F_{9/2}$, $^6H_{9/2}$+$^6F_{11/2}$, and $^6H_{11/2}$ upper-states, respectively.

Following the ICP-AES results, the segregation coefficient of Dy^{3+} in each crystal is calculated as the ratio of its concentration in the crystal and melt. Obtained results are given in Table 1. The effective segregation coefficient of Dy^{3+} in each crystal is about 0.48, which is in agreement with the previous report[21].

Next, absorption cross-section (σ_{abs}) at 447 nm is obtained using the formula:

$$\sigma_{abs} = \alpha / N_c \quad (1)$$

Where α is absorption coefficient and N_c is the amount of Dy^{3+} ions per cm^3.

The σ_{abs} of Dy^{3+} in YAG is ~1.6×10^{-21} cm^2 as presented in Table 1. The theoretical and experimental line-strengths of Dy: YAG are obtained utilizing J-O theory[26-27]:

$$S_{cal}(J \to J') \sum_{t=2,4,6} \Omega_t |\langle S,L,J \| U^{(t)} \| S',L',J' \rangle|^2 \quad (2)$$

$$S_{exp}(J \to J') = \frac{27hc(2J+1)n}{8\pi^3 e^2 N_c (n^2+2)^2 \bar{\lambda} L} \int \alpha(\lambda) d\lambda \quad (3)$$

Where $\Omega_{t(t=2,4,6)}$ are the J-O intensity parameters, and Ω_2 is related to the symmetry of Dy^{3+} and the chemical bond between Dy^{3+} and O^{2-}. Here, $\| U^{(t)} \|$ is the squared reduced matrix elements of the tensorial operator, which has been calculated by Carnall in Ref. [28]. n is refractive indices which are calculated by the Sellmeier equation for YAG crystal[29]. The values of Planck constant (h), speed of light (c), and electron charge (e) are 6.626×10^{-27} erg·s (1 erg·s =10^{-7} J·s), 2.998×10^{10} cm·s^{-1}, and 4.803×10^{-10} esu (1 A=3×10^9 esu), respectively. $\bar{\lambda}$ is average wavelength of absorption band for $J \to J'$ transition, and L is length of the crystal in the light pass direction.

The value of root-mean-square (RMS) is evaluated as:

$$RMS = \sqrt{\sum_{J'} (S_{exp} - S_{cal})^2 / (N-3)} \quad (4)$$

Where S_{exp} and S_{cal} are the line-strengths of the experimental and theoretical data respectively, and N is the number of absorption bands used for calculation. The three J-O intensity parameters of the studied crystals are fitted and the above parameters are all given in Table 2.

Table 1 Concentration, effective segregation coefficient and absorption cross-section of Dy^{3+} in YAG crystal

Crystal	c/% (in atomic)	k_{eff}	N_c/cm^{-3}	α/cm^{-1}	σ_{abs}/cm^2
0.5% Dy: YAG	0.239	0.478	3.31×10^{19}	0.055	1.66×10^{-21}
1.0% Dy: YAG	0.479	0.479	6.61×10^{19}	0.103	1.56×10^{-21}
2.0% Dy: YAG	0.970	0.485	1.33×10^{20}	0.215	1.61×10^{-21}
3.0% Dy: YAG	1.427	0.475	1.95×10^{20}	0.338	1.73×10^{-21}
4.0% Dy: YAG	1.975	0.494	2.69×10^{20}	0.430	1.60×10^{-21}

Table 2　Experimental line strength, calculated line strength, and J-O intensity parameters of Dy: YAG crystals

$^6H_{15/2}$ →	$\bar{\lambda}$ /nm	n	0.5%Dy: YAG		1.0%Dy: YAG		2.0%Dy: YAG		3.0%Dy: YAG		4.0%Dy: YAG	
			S_{exp}/($\times10^{-20}$, cm^2)	S_{cal}/($\times10^{-20}$, cm^2)	S_{exp}/($\times10^{-20}$, cm^2)	S_{cal}/($\times10^{-20}$, cm^2)	S_{exp}/($\times10^{-20}$, cm^2)	S_{cal}/($\times10^{-20}$, cm^2)	S_{exp}/($\times10^{-20}$, cm^2)	S_{cal}/($\times10^{-20}$, cm^2)	S_{exp}/($\times10^{-20}$, cm^2)	S_{cal}/($\times10^{-20}$, cm^2)
$^4M_{17/2}$+$^6P_{3/2}$+ $^4G_{9/2}$+$^4I_{9/2}$	327	1.89	0.447	0.298	0.460	0.320	0.526	0.323	0.498	0.327	0.467	0.341
$^6P_{7/2}$+$^4I_{11/2}$	353	1.88	0.905	0.723	1.128	0.850	1.371	1.182	1.719	1.454	1.648	1.403
$^6P_{5/2}$+$^4M_{19/2}$	367	1.87	0.733	0.474	0.806	0.511	0.907	0.525	0.898	0.540	0.918	0.560
$^4K_{17/2}$+$^4M_{21/2}$+ $^4I_{13/2}$+$^4F_{7/2}$	387	1.86	0.651	0.729	0.723	0.793	0.801	0.854	0.851	0.908	0.873	0.925
$^4I_{15/2}$	451	1.85	0.257	0.178	0.253	0.191	0.187	0.191	0.213	0.192	0.227	0.199
$^6F_{3/2}$	755	1.82	0.217	0.158	0.189	0.170	0.202	0.171	0.225	0.173	0.205	0.181
$^6F_{5/2}$	804	1.82	1.083	0.909	1.140	0.975	1.266	0.983	1.252	0.996	1.228	1.039
$^6F_{7/2}$	908	1.82	2.07	2.057	2.361	2.226	2.243	2.328	2.462	2.426	2.565	2.502
$^6H_{7/2}$+$^6F_{9/2}$	1088	1.81	2.577	2.741	2.74	3.022	3.249	3.403	3.480	3.731	3.528	3.767
RMS/($\times10^{-20}$, cm^2)				0.180		0.230		0.237		0.246		0.226
$\Omega_{t(t=2,4,6)}$/($\times10^{-20}$, cm^2)				Ω_2=0.793 Ω_4=1.284 Ω_6=2.634		Ω_2=0.747 Ω_4=1.520 Ω_6=2.825		Ω_2=0.498 Ω_4=2.155 Ω_6=2.848		Ω_2=0.312 Ω_4=2.674 Ω_6=2.887		Ω_2=0.142 Ω_4=2.573 Ω_6=3.011

Later, J-O intensity parameters Ω_t are used to obtain the radiative transition rates from the excited state $^4F_{9/2}$ to lower states which comprise both electric dipole (A_{ed}) and magnetic dipole (A_{md}) transitions in some cases. A_{ed} and A_{md} values are computed using formulae:

$$A = A_{ed} + A_{md} \tag{5}$$

$$A_{ed}(J \to J') = \frac{64\pi^4 e^2 n(n^2+2)^2}{27h(2J+1)\lambda_a^3} \sum_{t=2,4,6} \Omega_t \,|\, S, L, J \,\|\, U^{(t)} \,\|\, S', L', J' \,|^2 \tag{6}$$

$$A_{md}(J \to J') = \frac{64\pi^4 e^2 n^3}{3h(2J+1)\lambda_a^3} S_{md} \tag{7}$$

Where A_{ed} and A_{md} are the radiative transition rates contributed by electric-dipole and magnetic-dipole transitions, respectively. Here, the emission transition matrix of Dy^{3+} ion $\| U^{(t)} \|$ and S_{md} values are quoted from Ref. [30].

The fluorescence branching ratios (β) and the radiative lifetime (τ_r) of the $^4F_{9/2}$ level in the investigated crystals are obtained using expressions:

$$\beta_{JJ'} = \frac{A(J \to J')}{\sum_{J'} A(J \to J')} \tag{8}$$

$$\tau_r = \frac{1}{\sum_{J'} A(J \to J')} \tag{9}$$

Spontaneous emission transition rate (A) and fluorescence branching ratio (β) of $^4F_{9/2}$ to lower levels are listed in Table 3. β of yellow emission which corresponds to $^4F_{9/2}$→$^6H_{13/2}$ transition is in the range of 46%–50% for Dy: YAG crystals, which indicates that the yellow emission has considerable potential value in them.

Table 3　Spontaneous emission transition rate (A) and fluorescence branching ratio (β) of Dy: YAG crystals

$^4F_{9/2}$→$^{2S+1}L_J$	0.5%Dy: YAG		1.0%Dy: YAG		2.0%Dy: YAG		3.0%Dy: YAG		4.0%Dy: YAG	
	A/s^{-1}	β/%	A/s^{-1}	β/%	A/s^{-1}	β/%	A/s^{-1}	β/%	A/s^{-1}	β/%
$^6F_{1/2}$	0.08	0.01	0.10	0.01	0.14	0.01	0.17	0.02	0.16	0.02
$^6F_{3/2}$	0.15	0.02	0.16	0.02	0.16	0.02	0.16	0.02	0.17	0.02
$^6F_{5/2}$	1.82	0.20	1.81	0.19	1.54	0.15	1.34	0.13	1.05	0.10
$^6F_{7/2}$	13.63	1.49	14.26	1.46	7.29	1.53	8.21	1.58	8.18	1.57
$^6H_{5/2}$	4.02	0.44	4.58	0.47	5.78	0.58	6.78	0.66	6.67	0.65
$^6H_{7/2}$ +$^6F_{9/2}$	54.73	5.96	59.10	6.04	49.39	6.71	56.13	7.19	55.44	7.10
$^6H_{9/2}$	17.78	1.94	18.84	1.93	15.42	1.98	16.34	2.02	16.13	1.99
$^6H_{11/2}$	43.30	4.72	44.21	4.52	25.93	4.26	24.99	4.06	23.05	3.85
$^6H_{13/2}$	456.91	49.79	483.85	49.46	482.81	48.22	486.21	47.34	479.08	46.58
$^6H_{15/2}$	325.23	35.44	351.44	35.92	365.79	36.54	379.80	36.98	392.16	38.13
τ_r/ms	1.090		1.022		0.999		0.974		0.972	

2.2 Fluorescent characteristics

Emission spectra of all samples under 447 nm excitation wavelength are shown in Fig. 3(a). Luminescence band peaks at 484, 582, 676, and 761 nm are corresponding to transitions from $^4F_{9/2}$ to $^6H_{15/2}$, $^6H_{13/2}$, $^6H_{11/2}$, and $^6H_{9/2}$+ $^6F_{11/2}$ lower levels, respectively. The luminescence intensity and the fitted $^4F_{9/2}$ level lifetime with different doping concentrations at 447 nm were plotted in Fig. 3(b).

Further, quantum efficiency (η) is defined by $\eta = \tau/\tau_r$, where, τ_r is $^4F_{9/2}$ level radiative lifetime, τ is $^4F_{9/2}$ level lifetime. The stimulated emission cross-section (σ_{em}) can be obtained by Füchtbauere Ladenburg formula[31-32] as:

$$\sigma_{em}(\lambda) = \frac{\lambda^5 I(\lambda) A(J \rightarrow J')}{8\pi n^2 c \int \lambda I(\lambda) \mathrm{d}\lambda} \quad (10)$$

Where λ, n, c, and $A(J \rightarrow J')$ have their usual meanings. The value of $\sigma_{em}\tau$ is calculated and it is inversely proportional to the laser threshold[33]. All related spectroscopic parameters are contrasted with other Dy^{3+} doped crystals. σ_{em} at 582 nm of as-grown Dy: YAG crystals are found to be in the range from 2.36×10^{-21} to 2.71×10^{-21} cm^2. The obtained results in all samples are listed in Table 4.

σ_{em} of 1.0%Dy: YAG is close to those of gallate and scandate crystals related value at a similar concentration while it is much smaller than those of sesquioxide and fluoride crystals[13-14, 34-36] respective values. From the $\sigma_{em}\tau$ product, it is noticed that Dy: YAG possesses a smaller threshold than Dy^{3+}: $Gd_3Ga_3Al_2O_{12}$, Dy^{3+}: $Gd_3Ga_5O_{12}$, and Dy^{3+}: $GdScO_3$ crystals. Fluoride crystals might have a lower threshold for yellow laser operation but due to adverse factors such as thermal effect and lower mechanical strength, it is difficult to develop high-power lasers[18-19]. η of Dy: YAG declines rapidly with Dy^{3+} doping content increment, which is a sign of non-radiative transitions existence between Dy^{3+} ions, so it is not suitable to generate lasing action with Dy: YAG crystal at higher doping levels. Among all crystals, 1.0% Dy: YAG has the largest σ_{em} as well as $\sigma_{em}\tau$ for 582 nm yellow emission. Among five samples, the 1.0% Dy: YAG crystal also shows an intense fluorescence intensity with the 447 nm excitation with a longer decay time of 0.823 ms, which is close to the previous work[37]. The fluorescence intensity and σ_{em} of 2.0% Dy: YAG are slightly less than that of 1.0% Dy: YAG, but 2.0%Dy: YAG has a higher α. Hence, 1.0%Dy: YAG and 2.0%Dy: YAG crystals are the suitable candidates for the generation of yellow laser output.

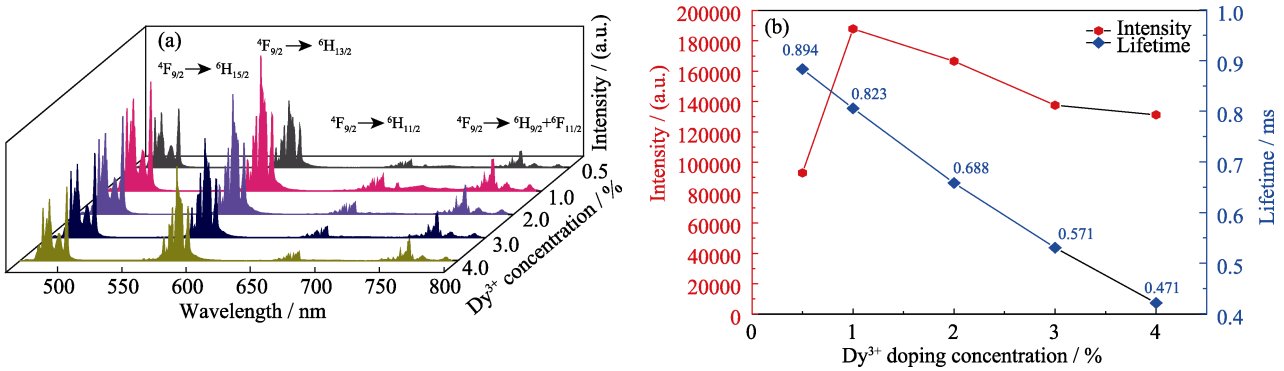

Fig. 3 Emission spectra of YAG crystals with different Dy^{3+} concentrations excited by 447 nm (a) and variation of intensity of 582 nm and $^4F_{9/2}$ level lifetime with Dy^{3+} concentrations in Dy: YAG crystals (b)

Table 4 Emission property parameters of Dy^{3+} in YAG and other crystals

Crystal	$\tau_r(^4F_{9/2}$ level)/ms	$\tau(^4F_{9/2}$ level)/ms	σ_{em} for yellow emission/($\times10^{-21}$, cm^2)	$\sigma_{em}\tau$/($\times10^{-21}$, cm^2·ms)	η/%	Ref.
0.5%Dy: YAG	1.090	0.894	2.36	2.110	82.02	This work
1.0%Dy: YAG	1.022	0.823	2.71	2.230	80.53	
2.0%Dy: YAG	0.999	0.688	2.66	1.830	68.87	
3.0%Dy: YAG	0.974	0.571	2.54	1.450	58.62	
4.0%Dy: YAG	0.972	0.471	2.49	1.170	48.46	
1.0%Dy^{3+}: $Gd_3Ga_3Al_2O_{12}$	0.596	0.573	3.20	1.834	96.14	[13]
3.0%Dy^{3+}: Lu_2O_3	0.756	0.112	7.10	7.952	14.80	[14]
2.0%Dy^{3+}: CeF_3	3.747	1.530	9.259	0.1417	40.83	[17]
1.0%Dy^{3+}: $GdScO_3$	0.650	0.459	4.10	1.882	70.60	[34]
2.0%Dy^{3+}: $Gd_3Ga_5O_{12}$	1.107	0.790	2.62	2.070	71.40	[35]
2.0%Dy^{3+}: LaF_3	1.700	1.370	7.00	9.590	80.59	[36]

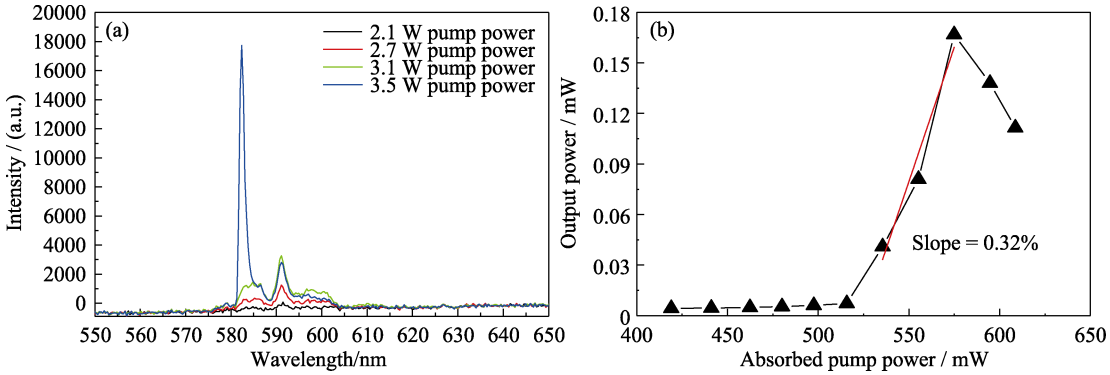

Fig. 4　Laser spectra (a) and variation of output power with absorbed pump power of 2.0%Dy: YAG crystal (b)

2.3　Laser performance

The continuous wave (CW) yellow laser output was obtained in 2.0%Dy: YAG crystal. Fig. 4(a) shows the laser spectra of Dy: YAG crystal. The central wavelength of the laser is 582.5 nm, and the full width at half maximum is 1.2 nm. Fig. 4(b) shows the relation curve between absorption pump power and output power, and the maximum output power is 166.8 μW. The slope efficiency is calculated to be 0.32%, with the maximum output power of 0.029%. The laser operation threshold is around 535 mW, which is higher than that of Dy^{3+},Tb^{3+}:$LiLuF_4$ (320 mW)[38]. When the input power exceeds 3382 mW, the output power decreases significantly which is mainly due to the degradation of rare earth ions caused by laser thermal effect. Owing to the laser experiment parameters haven't been optimized, the laser output power and efficiency are still very low, we are trying to improve the laser output power now.

3　Conclusions

The visible fluorescence features of Dy: YAG crystals with different Dy^{3+} doping concentrations were analyzed thoroughly. The optimum concentration for yellow emission under 447 nm is 1.0%, and the $^4F_{9/2}$ level lifetime is calculated to be 0.823 ms. 1.0%Dy: YAG has the largest σ_{em} at 582 nm in present work. 2.0%Dy: YAG could also be an alternative crystal for yellow lasing action on consideration of its greater yellow emission intensity and σ_{em}, the acceptable lifetime of $^4F_{9/2}$ level, and higher absorption intensity. Hence, 1.0%Dy: YAG and 2.0%Dy: YAG crystals are potential candidates for yellow laser output. Finally, the CW laser with the maximum output power of 166.8 μW yellow laser operation is obtained based on 2.0%Dy: YAG crystal.

References:

[1] LI N, LIU B, SHI J J, *et al*. Research progress of rare-earth doped laser crystals in visible region. *Journal of Inorganic Materials*, 2019, **34(6):** 573.

[2] SHI Z X, WANG J, GUAN X. Multicolor upconversion emission tuning of $NaY(WO_4)_2$: Dy^{3+} *via* Er^{3+} doping. *Journal of Inorganic Materials*, 2018, **33(5):** 521.

[3] WANG Z J, LI P L, YANG Z P, *et al*. Luminescence characteristics of Dy^{3+} activated $LiCaBO_3$ phosphor. *Journal of Inorganic Materials*, 2009, **24(5):** 1069.

[4] WANG M L, XU J Y, ZHANG Y, *et al*. Growth and thermo-luminescence properties of Dy: $Bi_4Si_3O_{12}$ crystals. *Journal of Inorganic Materials*, 2016, **31(10):** 1068.

[5] CAVALLI E. Optical spectroscopy of Dy^{3+} in crystalline hosts: general aspects, personal considerations and some news. *Optical Materials X*, 2019, **1:** 100014.

[6] KRÄNKEL C, MARZAHl D T, MOGLIA F, *et al.* Out of the blue: semiconductor laser pumped visible rare-earth doped lasers. *Laser & Photonics Rev.*, 2016, **10:** 10548.

[7] TEMIZ S A, ATASEVEN A, DURSUN R, *et al.* Successful treatment of poikiloderma of Civatte with a 577 nm pro-yellow laser. *J. Cosmet. Dermatol.*, 2020, **19:** 2769.

[8] UZLU D, ERDÖL H, KOLA M, *et al.* The efficacy of subthreshold micropulse yellow laser (577 nm) in chronic central serous chorioretinopathy. *Laser Med. Sci.*, 2020, **12:** 981.

[9] PIZZOCARO M, COSTANZO G A, GODONE A, *et al.* Realization of an ultrastable 578 nm laser for an Yb lattice clock. *IEEE T. Ultrason. Ferr.*, 2012, **59:** 426.

[10] ZONG Q S, BIAN Q, MA H D, *et al.* The research progress of the new sodium beacon laser. *Laser Technol.*, 2020, **44:** 404.

[11] BOWMAN S R, O'CONNOR S, CONDON N J. Diode pumped yellow dysprosium lasers. *Opt. Express*, 2012, **20:** 12906.

[12] CAI XIUYUAN, WANG YAN, LI JIANFU, *et al.* Thermal, and optical features study of Dy:$YAlO_3$ and Dy/Tb:$YAlO_3$ crystals for yellow laser applications. *J. Lumin.*, 2020, **231:** 117711.

[13] LISIECKI R, SOLARZ P, NIEDŹWIEDZKI T, *et al.* $Gd_3Ga_3Al_2O_{12}$ single crystal doped with dysprosium spectroscopic properties and luminescence characteristics. *J. Alloys Compd.*, 2016, **689:** 733.

[14] SHI J J, LIU B, WANG Q G, *et al.* Crystal growth, spectroscopic characteristics, and Judd-Ofelt analysis of Dy:Lu_2O_3 for yellow laser. *Chin. Phys. B*, 2018, **27:** 077802.

[15] CHEN H, LOISEAU P, AKA G. Optical properties of Dy^{3+}-doped $CaYAlO_4$ crystal. *J. Lumin.*, 2018, **199:** 509.

[16] JIANG T, GONG X, CHEN Y, *et al.* Spectroscopic properties of Dy^{3+}-doped $NaBi(WO_4)_2$ crystal. *J. Lumin.*, 2019, **210:** 83.

[17] YANG Y, ZHANG L, LI S, *et al.* Crystal growth and 570 nm emission of Dy^{3+} doped CeF_3 single crystal. *J. Lumin.*, 2019, **215:** 116707.

[18] METZ P W, MOGLIA F, REICHERT F, *et al.* Novel Rare Earth Solid State Lasers with Emission Wavelengths in the Visible Spectral Range. Lasers and Electro-Optics Europe, Munich,

Germany, 2013: 1.
[19] BOLOGNESI G, PARISI D, CALONICO D, *et al.* Yellow laser performance of Dy^{3+} in co-doped Dy,Tb:$LiLuF_4$. *Opt. Lett.*, 2014, **39:** 6628.
[20] JU Q J, SHEN H, YAO W M, *et al.* Laser diode pumped Dy: YAG yellow laser. *Chin. J. Lasers*, 2016, **43:** 0815002.
[21] PAN Y X, ZHOU S D, LI D Z, *et al.* Growth and optical properties of Dy:$Y_3Al_5O_{12}$ crystal. *Physica B Condens. Matter*, 2018, **530:** 317.
[22] XU J, SONG Q S, LIU J, *et al.* Spectroscopic characteristics of Dy^{3+}-doped $Y_3Al_5O_{12}$ (YAG) and $Y_3ScAl_4O_{12}$ (YSAG) garnet single crystals grown by the micro-pulling-down method. *J. Lumin.*, 2019, **215:** 116675.
[23] YU H, SU L G, QIAN X B, *et al.* Influence of Gd^{3+} on the optical properties of Dy^{3+}-activated CaF_2 single crystal for white LED application. *J. Electron. Mater.*, 2019, **48:** 2910.
[24] XU F, FANG L Z, ZHOU X, *et al.* Multi-color emission of Dy^{3+}/Eu^{3+} co-doped $LiLuF_4$ single crystals for white light-emitting devices. *Opt. Mater.*, 2020, **108:** 110222.
[25] DING S J, LI H Y, REN H, *et al.* Ultra-broad absorption band of a Dy^{3+}-doped $Gd_3Sc_2Al_3O_{12}$ garnet crystal at around 450 nm: a potential crystal for InGaN LD-pumped all-solid-state yellow laser. *CrystEngComm*, 2021, **23:** 5481.
[26] JUDD B R. Optical absorption intensities of rare-earth ions. *Physical Review*, 1962, **127:** 750.
[27] OFELT G S. Intensities of crystal spectra of rare earth ions. *Journal of Chemical Physics*, 1962, **37:** 511.
[28] CARNALL W T, FIELDS P R, RAJNAK K. Electronic energy levels in the trivalent lanthanide aquo ions. I. Pr^{3+}, Nd^{3+}, Pm^{3+}, Sm^{3+}, Dy^{3+}, Ho^{3+}, Er^{3+}, and Tm^{3+}. *Chemical Physics*, 1968, **49:** 4424.
[29] ZELMON D E, SMALL D L, PAGE R. Refractive-index measurements of undoped yttrium aluminum garnet from 0.4 to 5.0 μm. *Appl. Opt.*, 1998, **37:** 4933.
[30] JAYASANKAR C K, RUKMINI E. Spectroscopic investigations of Dy^{3+} ions in borosulphate glasses. *Physica B*, 1997, **240:** 273.
[31] MCCAMY C S. Correlated color temperature as an explicit function of chromaticity coordinates. *Color Res. Appl.*, 1992, **17:** 142.
[32] AULL B F, JENSSEN H P. Vibronic interactions in Nd:YAG resulting in nonreciprocity of absorption and stimulated emission cross sections. *IEEE .Quantum Elect.*, 1982, **18:** 925.
[33] LIU J, SONG Q S, LI D Z, *et al.* Crystal growth and spectroscopic characterization of Sm:$LaMgAl_{11}O_{19}$ crystal . *J. Lumin.*, 2019, **215:** 116701.
[34] FANG P, LIU W P, ZHANG Q L, *et al.* Growth, structure, and spectroscopic characteristics of a promising yellow laser crystal Dy:$GdScO_3$. *Lumin.*, 2018, **201:** 176.
[35] WANG Y, YOU Z Y, LI J F, *et al.* Optical properties of Dy^{3+} ion in GGG laser crystal. *Phys. D Appl. Phys.*, 2010, **43:** 075402.
[36] LI S M, ZHANG L H, ZHANG P X, *et al.* Spectroscopic characterizations of Dy:LaF_3 crystal. *Infrared Phys. Techn.*, 2017, **87:** 65.
[37] BOWMAN S R, CONDON N J, O'CONNOR S, *et al.* Diode-pumped Dysprosium Laser Materials. SPIE Defense, Security, and Sensing, Orlando, Florida, United States, 2009.
[38] BOLOGNESI G, PARISI D, CALONICO D, *et al*. Yellow laser performance of Dy^{3+} in co-doped Dy,Tb:$LiLuF_4$. *Optics Letters*, 2014, **39:** 6628.

Dy^{3+}: $Y_3Al_5O_{12}$ 晶体的光谱与黄色激光性能

杨佳雪[1,2], 李 雯[1,3], 王 燕[1,4], 朱昭捷[1,4], 游振宇[1,4],
李坚富[1,4], 涂朝阳[1,4]

(1. 中国科学院 福建物质结构研究所, 福州 350002; 2. 福州大学 化学学院, 福州 350116; 3. 福州大学 材料科学与工程学院, 福州 350116; 4. 中国福建光电信息科学与技术创新实验室(闽都创新实验室), 福州 350108)

摘 要: 近年来, 黄色激光晶体在激光显示、激光医疗、激光雷达(光探测和测距)、玻色-爱因斯坦凝聚、原子冷却和俘获等领域具有广泛的应用, 吸引了研究人员极大的兴趣。随着蓝光 LD 泵浦源的商用化, 直接泵浦 Dy^{3+}掺杂激光晶体可输出黄色激光, 对应 $^4F_{9/2}\rightarrow{}^6H_{13/2}$ 跃迁。本工作采用提拉法生长了 Dy^{3+}掺杂浓度分别为 0.5%、1.0%、2.0%、3.0%和 4.0%(原子分数)的 Dy^{3+}: $Y_3Al_5O_{12}$(Dy:YAG)晶体, 并分析了晶体开裂的原因。基于 Judd-Ofelt 理论计算了 J-O 强度参数, 并利用其评估了不同掺杂浓度的 Dy:YAG 晶体的其它激光参数。综合讨论了 Dy^{3+}掺杂浓度对荧光分支比、受激发射截面、量子效率等光谱性能的影响。在五个晶体样品中, 1.0%Dy: YAG 晶体在 447 nm 激发下实现了 582 nm 最大的受激发射截面值和最强的荧光强度值, 荧光寿命较长, 达到 0.823 ms。与之相比, 2.0%Dy: YAG 晶体发射参数值略低, 但是其吸收系数更大。研究结果表明, 激光二极管泵浦的 Dy:YAG 黄色激光晶体中 Dy^{3+}离子的浓度为 1.0%和 2.0%较为合适, 并基于 2.0%Dy: YAG 晶体实现了连续黄色激光输出, 最大功率为 166.8 μW, 激光峰值波长为 582.5 nm。

关 键 词: YAG 晶体; Dy^{3+}; 晶体生长; 荧光特性; 黄色激光

中图分类号: TN244 **文献标志码:** A